Biochemical and Biophysical Research Communications 677 (2023) 162–167

Contents lists available at ScienceDirect

Biochemical and Biophysical Research Communications

journal homepage: www.elsevier.com/locate/ybbrc

The importance of proteasome grip depends on substrate stability

Destini A. Stanton, Emily A. Ellis, Mariah R. Cruse, Rafael Jedlinski, Daniel A. Kraut *

Department of Chemistry, Villanova University, Villanova, PA, 19085, USA

ARTICLE INFO

Keywords:
Proteasome
ATP-dependent protease
Protein unfolding
Protein degradation

ABSTRACT

The 26S proteasome is responsible for the unfolding and degradation of intracellular proteins in eukaryotes. A hexameric ring of ATPases (Rpt1-Rpt6) grabs onto substrates and unfolds them by pulling them through a central pore and translocating them into the 20S degradation chamber. A set of pore loops containing a so-called aromatic paddle motif in each Rpt subunit is believed to be important for the proteasome's ability to unfold and translocate substrates. Based on structural and mechanistic experiments, paddles from adjacent Rpt subunits, which are arrayed in a spiral staircase conformation, grip and pull on the substrate in a hand-over-hand type mechanism, disengaging at the bottom of the staircase and re-engaging at the top. We tested the contribution of the aromatic paddles to unfolding substrates of differing stabilities by mutating the paddles singly or in combination. For an easy-to-unfold substrate (a circular permutant of green fluorescent protein; GFP), mutations had little effect on degradation rates. For a substrate with moderate stability (enhanced GFP), there were modest effects of individual mutations on GFP unfolding rates, and alternating aromatic paddle mutants had a larger detrimental effect on unfolding than sequential mutants. For a more stable substrate (superfolder GFP), unfolding is overall slower, and multiple simultaneous mutations essentially prevent unfolding. Our results highlight the context-dependent need for grip during unfolding, support the hand-over-hand model for substrate unfolding and translocation, and suggest that for hard-to-unfold substrates, it is important to have simultaneous strong contacts to the substrate for unfolding to occur. The results also suggest a kinetic proofreading model, where substrates that cannot be easily unfolded are instead clipped, removing the initiation region and preventing futile unfolding attempts.

1. Introduction

All organisms contain ATP-dependent proteases, which are responsible for the unfolding and degradation of intracellular proteins [1]. In eukaryotes, this function is taken on by the 26S proteasome [2,3]. Proteins to be degraded are typically tagged with a polyubiquitin chain, which then docks onto one of several ubiquitin receptors associated with the proteasome's 19S regulatory particle (Fig. 1A). Degradation begins when an unstructured region of the substrate protein is engaged by a ring of ATP-dependent motor proteins (Rpt1-Rpt6) at the base of the 19S. Engagement leads to a conformational change that aligns the regulatory particle with the 20S core particle, allowing ATP-dependent unfolding of the substrate followed by translocation of the unfolded substrate into the 20S, which contains protease active sites that cleave the substrate into small peptides. During the translocation process, the ubiquitin chain on the substrate is removed by the deubiquitinase Rpn11 enabling the recycling of ubiquitin.

Each Rpt subunit contains a region called pore loop 1 or the aromatic paddle (because of its central tyrosine residue) that extends into the pore formed by the Rpt subunits at the base of the 19S. The aromatic paddle-containing loops are arranged in a spiral staircase (Fig. 1B) whose arrangement alters depending on the conformation of the proteasome [4]. The aromatic paddles directly contact the substrate and, in response to ATP hydrolysis, are believed to transmit the force that leads to both unfolding and translocation. Based on recent Cryo-EM structures of substrate-translocating proteasomes, a "hand-over-hand" model has been proposed, whereby each paddle contacting the substrate moves downwards until it reaches the bottom of the staircase, at which point it disengages, moves back up to the top of the staircase, and re-engages the substrate [5,6].

Aromatic paddles are conserved in ATP-dependent proteases and unfoldases (members of the AAA+ ATPase family). Bacterial ATP-dependent unfoldases, unlike the proteasome, form a homohexameric ring, and mutation of the central aromatic residue (typically tyrosine or

* Corresponding author.
E-mail address: daniel.kraut@villanova.edu (D.A. Kraut).

https://doi.org/10.1016/j.bbrc.2023.08.025
Received 4 August 2023; Accepted 11 August 2023
Available online 12 August 2023

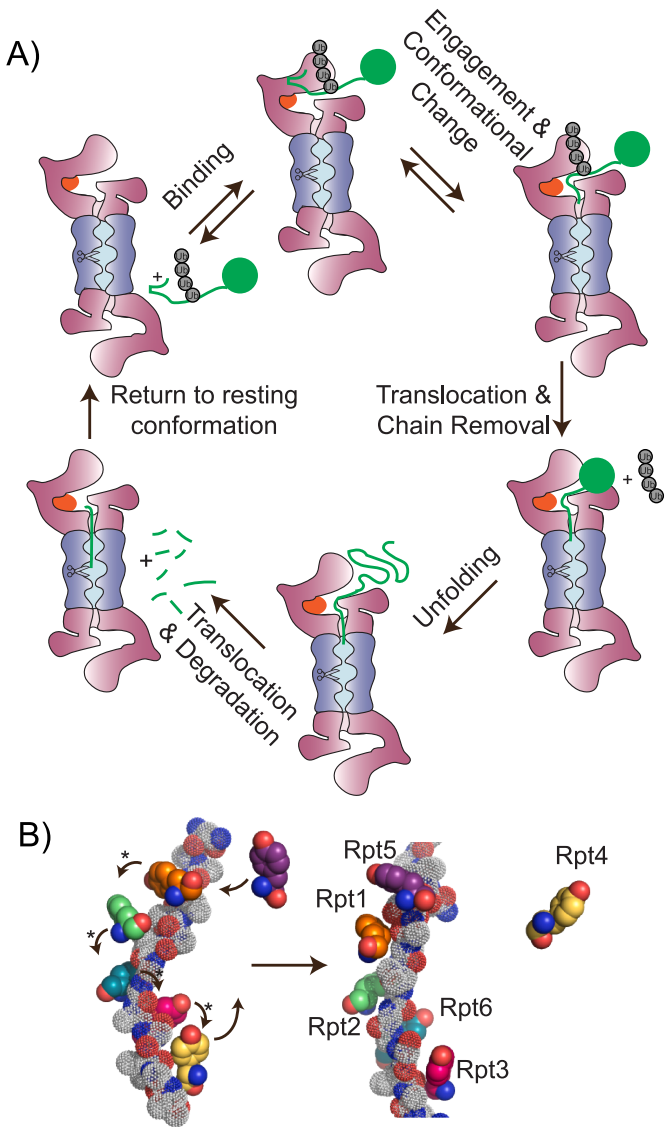

Fig. 1. Mechanism of proteasomal degradation. **A)** Degradation cycle, in which a polyubiquitinated substrate (green) binds via ubiquitin receptors, an unstructured region engages the motor proteins, leading to conformational change, translocation, ubiquitin chain removal by Rpn11 (orange), unfolding, translocation and degradation. **B)** Hand-over-hand model for translocation. Aromatic paddle tyrosines from five subunits contact the substrate (backbone shown as dots). The unengaged subunit (Rpt5 in this case) binds to the top of the substrate as the other pore loops move downwards (arrows; * indicates movement while in contact with substrate which would be expected to generate force) while the lowest subunit (Rpt4 in this case) disengages. In the next cycle, Rpt4 will engage at the top of the substrate and Rpt3 will disengage. From PDB ID 6EF2 (left) and 6EF3 (right). (For interpretation of the references to colour in this figure legend, the reader is referred to the Web version of this article.)

phenylalanine) cripples the enzyme, preventing unfolding or degradation from occurring [7–11]. In the bacterial ATP-dependent protease ClpXP, a single-chain ClpX was created, allowing for individual and combinations of aromatic paddle substitutions to test the motor protein's grip on various substrates [12]. The effects of mutations were substrate dependent, with more difficult to unfold GFP substrates showing larger effects on degradation rates. There were additional positional effects of mutations, with, for example, three mutant subunits followed by three wild-type subunits having a smaller effect than alternating wild-type and mutant subunits, suggesting that adjacent wild-type pore loops are important for ClpX's unfolding ability. In the 26S proteasome, each of the six Rpt subunits are unique, allowing for mutation in an otherwise wild-type proteasome. Interestingly, in the two studies where each individual aromatic paddle tyrosine was mutated, somewhat different results were obtained [13,14]. In one experiment, a ubiquitinated titin substrate was degraded at rates between ~40% and 200% of wild-type by different Rpt mutants, with a Rpt4 tyrosine to alanine (YA) mutant having the largest negative effect, Rpt6YA having no effect, and Rpt1YA and Rpt2YA mutants accelerating degradation [13]. A different experiment (using reconstituted proteasome) concluded that all mutants had a detrimental effect on degradation of a ubiquitinated GFP-titin fusion protein, with rates between ~50% (Rpt2YA) and 90% (Rpt6YA) of wild-type [14]. In both cases the rates being measured represented overall rates of degradation, which includes engagement, conformational change, unfolding and translocation.

We set out to address the question of how individual and combinations of Rpt YA mutants affect the proteasome's grip on substrates by determining not just overall degradation rates but also by directly measuring rates of substrate unfolding for substrates with varying stability. Our results highlight the substrate-dependent need for grip during unfolding, support the hand-over-hand model for substrate unfolding and translocation, and suggest that for hard to unfold substrates, it is important to have simultaneous strong contacts to the substrate for unfolding to occur.

2. Materials and methods

2.1. Constructs

Centromeric yeast plasmids encoding Rpt1-Rpt6 between the 5′ and 3′ UTRs of yeast Rpt1 containing either the Leu2 or Ura3 genes were a gift from Dan Finley [15]. Rpt YA mutations (Rpt1 Y283A, Rpt2 Y256A, Rpt3 Y246A, Rpt4 Y255A, Rpt5 Y225A, Rpt6 Y222A) were constructed in Leu2 containing plasmids using oligo-directed mutagenesis and confirmed by Sanger sequencing.

Cas9/gRNA constructs targeting locations within each Rpt subunit near the aromatic paddle tyrosine were constructed based on pML104 [16] (Addgene #67638) using PCR and confirmed by Sanger sequencing.

Plasmids are listed in Supplementary Table S1; sequences are available upon request.

2.2. Yeast strains

Yeast strains with each individual Rpt gene knocked out and covered by a WT gene in a Leu2 centromeric plasmid were a gift from Dan Finley [15]. Plasmids were replaced with the Ura3 containing plasmids, and a 3X-FLAG tag was added to the C-terminus of Rpn11 using PCR-directed homologous recombination [17]. Plasmid shuffling using selection with 5-fluoroorotic acid was used to replace wild-type Rpt1-Rpt6 Ura3 plasmids with mutant Leu2 plasmids to create single-mutant YA strains. Wild-type Rpt1 on a Ura3 plasmid was used for a wild-type control.

To create multiple mutations, CRISPR was used. A Cas9/gRNA construct targeting an individual Rpt subunit along with a PCR product of the mutant Rpt were co-transformed into a single-mutant strain. Targeted Rpt genes were sequenced to confirm mutations. After removal of the Cas9/gRNA plasmid by 5-fluoroorotic acid selection, additional mutagenesis was conducted to create triple mutants.

Strains are listed in Supplementary Table S2.

2.3. Protein purification

Proteasome substrates UBL-cp8sGFP-102-His_6, UBL-eGFP-102-His_6 and UBL-sGFP-102-His_6 were purified as described previously via NiNTA chromatography [18].

Yeast proteasome was purified as described previously via anti-FLAG affinity chromatography [19].

2.4. Degradation assays

Degradation assays were carried out essentially as described previously [18]. 100 nM proteasome and 20 nM substrate were incubated at 30 °C in degradation buffer (50 mM TrisCl, 5 mM $MgCl_2$, 5% (v/v) glycerol, 1 mM ATP, 10 mM creatine phosphate, 0.1 mg/mL creatine kinase, 1 mg/mL BSA, 0.1% Tween-20, and 1% DMSO, pH 7.5). At designated time points, samples were removed and placed into SDS-PAGE loading buffer to quench the reaction; samples remained unheated to prevent GFP denaturation. Gels were imaged on a Typhoon FLA 9500 using GFP fluorescence and analyzed using ImageQuant (Cytiva). Band intensities were normalized to full-length substrate at the initial 10" time point. The total fluorescence was determined by adding the full-length and fragment amounts, as no other appreciable fluorescent bands were detected.

2.5. Kinetic modeling

Kinetic modeling was carried out using COPASI software [20]. Binding and release steps were assigned rate constants as described previously [18].

2.6. ATPase assays

ATPase activity was measured using a coupled pyruvate kinase/lactate dehydrogenase assay. Reactions contained 20 nM proteasome, 6.8 units/mL pyruvate kinase, 9.9 units/mL lactate dehydrogenase, 0.4 mM NADH, 2 mM phosphoenolpyruvate, 0.5 mM DTT, and 0.5 mM ATP in a buffer consisting of 50 mM TrisCl pH 7.5, 5 mM $MgCl_2$, 5% (v/v) glycerol, and 0.1% Tween-20. Reaction was monitored at 340 nm at 30 °C in a 384 well plate using a BioRad Benchmark Plus UV–Vis platereader.

3. Results

We initially generated a set of yeast strains containing individual aromatic paddle tyrosine to alanine (YA) mutations (Supplementary Table S2) using a plasmid shuffling approach in which each strain has a centromeric plasmid containing the mutant Rpt gene driven by the Rpt1 promotor covering a chromosomal deletion of the wild-type gene [15]. A control strain (hereafter WT) contained a wild-type Rpt1 plasmid covering an Rpt1 chromosomal deletion. We then introduced additional YA mutations using CRISPR [16] (Supplementary Table S2). We generated three triple-mutant proteasomes with different spacings between mutant subunits: Rpt1/3/4 YA has a YA/WT/WT/YA/YA/WT pattern (2/1), Rpt1/4/6 YA has alternating YA and WT subunits

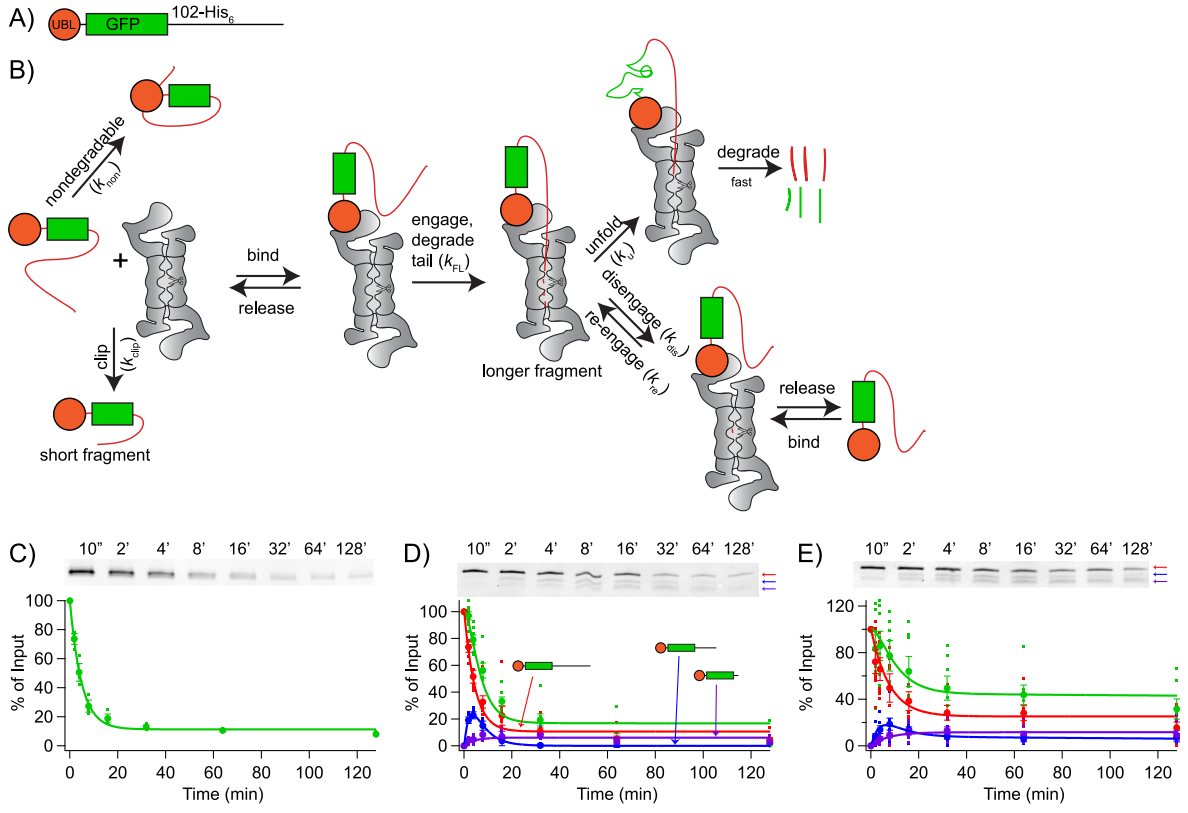

Fig. 2. Degradation of GFP-containing substrates with varying stabilities by WT yeast proteasome. **A**) Domain organization. **B**) Kinetic model for degradation of GFP substrates. Substrate is bound via the UBL, engaged, partially degraded to produce a longer fragment, which can either be unfolded and completely degraded or can alternatively be released and rebound repeatedly until it is degraded. Alternatively, substrate can be clipped, forming a shorter fragment, in a UBL-independent, proteasome-dependent process. **C**) Degradation of 20 nM UBL-cp8sGFP-102-His_6 by 100 nM WT yeast proteasome. Representative gel shows disappearance of full-length protein; no smaller GFP-containing fragments were observed. Dots are results from individual experiments, and closed circles and error bars represent the SEM of 3 experiments. Curve is a global fit of individual experiments to a single exponential. **D**) Degradation of 20 nM UBL-eGFP-102-His_6 by 100 nM WT yeast proteasome. Representative gel shows disappearance of full-length protein (red arrow) and appearance of longer (blue arrow) and shorter (purple arrow) clipped protein. The amounts of full-length protein (red circles), longer partially degraded protein (blue circles), shorter clipped protein (purple circles), and total fluorescence (green circles) are shown as a percentage of the full-length substrate present at the beginning of the reaction. Dots are results from individual experiments, and error bars represent the SEM of 7 experiments. Curves are from kinetic modeling to the scheme in **B** as described in **Methods**. **E**) Degradation of 20 nM UBL-sGFP-102-His_6 by 100 nM WT yeast proteasome as in **D**; n = 5. (For interpretation of the references to colour in this figure legend, the reader is referred to the Web version of this article.)

(alternating), and Rpt1/2/6 YA has three sequential YA and then three sequential WT subunits (sequential). Proteasome was than purified using a 3X-FLAG tag appended to the Rpn11 protein [19,21]. All proteasome preparations appeared intact vis SDS-PAGE (Supplementary Fig. S1).

We then presented the proteasome with a series of green fluorescent protein (GFP) substrates containing, from greatest to least stability, superfolder GFP (sGFP), enhanced GFP (eGFP) or a circular permutant of GFP (cp8sGFP). All substrates contained an N-terminal ubiquitin-like domain (UBL) for proteasomal targeting, a GFP domain, and a C-terminal unstructured region for initiation of degradation (Fig. 2A) [18]. We had previously shown that degradation of sGFP and eGFP-containing substrates proceeds through partially degraded GFP-containing intermediates, with irreversible ATP-independent tail clipping in competition with unfolding and degradation (Fig. 2B), while cp8sGFP-containing substrates were degraded without detectable intermediates or side products [18]. Kinetic modeling then allows for the direct determination of GFP unfolding rates for sGFP and eGFP substrates.

For WT proteasome, as expected cp8sGFP was degraded without apparent release of GFP-containing fragments (Fig. 2C), while eGFP (Fig. 2D) and sGFP (Fig. 2E) were largely unfolded and degraded, but with some transient production of longer GFP-containing products (blue, Fig. 2D and E) and some production of shorter clipped GFP-containing products (purple, Fig. 2D and E) that were stable on the time-scale of our assays. The least stable cp8sGFP substrate was degraded with an overall k_{obs} of 0.21 ± 0.02 min^{-1}, which potentially includes contributions from binding, engagement, unfolding and translocation. Single exponential fits to the full-length eGFP and sGFP substrates gave similar rate constants (Supplementary Table S3; 0.17 ± 0.02 and 0.14 ± 0.04 min^{-1}), suggesting that the initial steps of degradation are similar for all three substrates, and indicating that unfolding of cp8sGFP is unlikely to be rate limiting for degradation. From kinetic modeling, we extracted both an "initial" rate constant (engagement and initial tail degradation; k_{FL}) and an unfolding rate (k_u) for both eGFP and sGFP substrates (Supplementary Table S3), 0.37 ± 0.03 and 0.38 ± 0.06 min^{-1} for eGFP and 0.16 ± 0.01 and 0.23 ± 0.03 min^{-1} for sGFP respectively. As expected, eGFP was unfolded about two times more rapidly than the more stable sGFP (k_u). k_{FL} was also higher for eGFP than for sGFP, perhaps indicating that transient unfolding events could

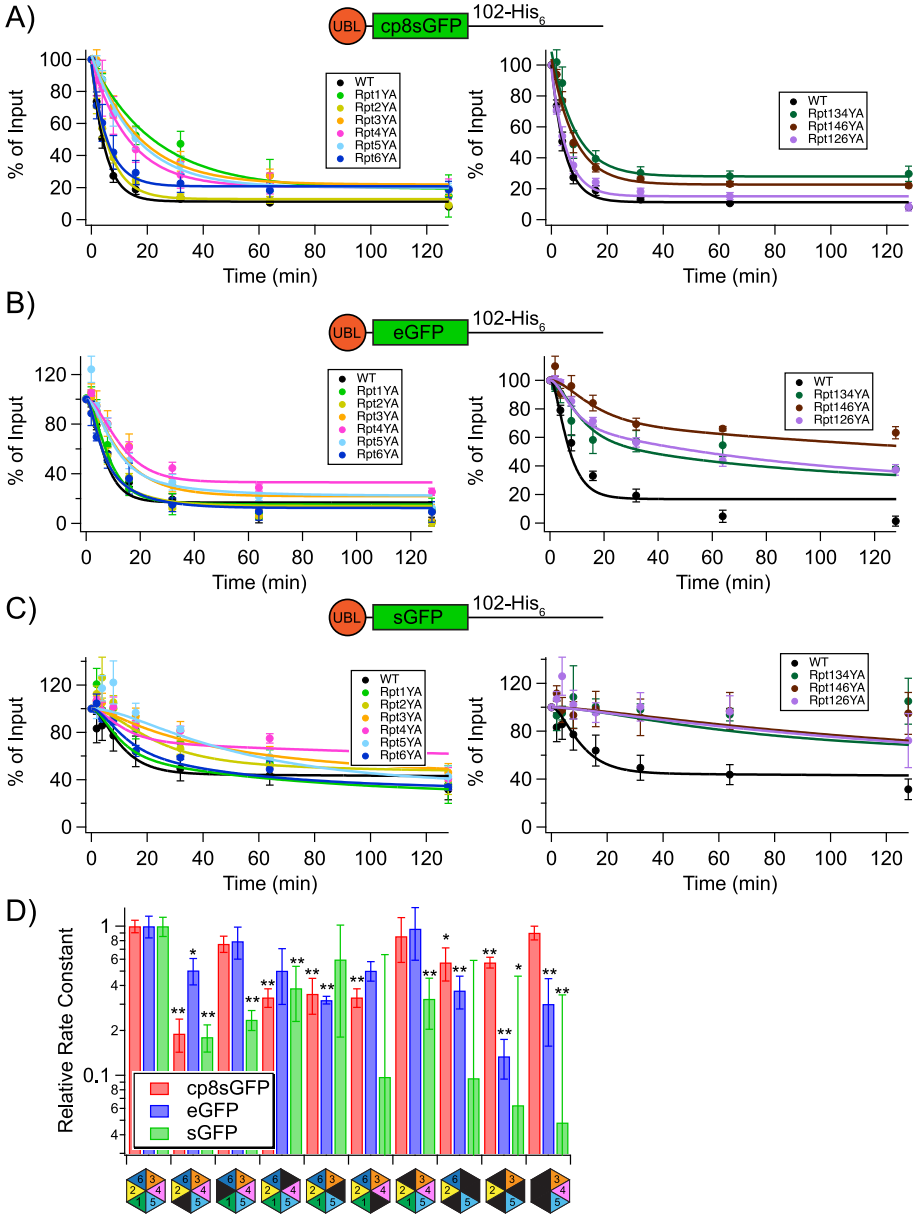

Fig. 3. Degradation of GFP substrates with varying stabilities by mutant proteasomes. **A**) Degradation (disappearance of total fluorescence) of 20 nM UBL-cp8sGFP-102-His_6 by 100 nM yeast proteasome for single (left) and triple (right) mutants. Closed circles and error bars represent the SEM of 3–6 experiments. Curve is a global fit to a single exponential. Full data for mutants shown in Supplementary Fig. S2. **B**) Degradation of 20 nM eGFP-102-His_6 by 100 nM yeast proteasome. Closed circles and error bars represent the SEM of 3–8 experiments. Curves are from kinetic modeling to the scheme in Fig. 2B. Full data for mutants shown in Supplementary Fig. S3. **C**) Degradation of 20 nM UBL-sGFP-102-His_6 by 100 nM WT yeast proteasome as in **B**; n = 3–5. Full data for mutants shown in Supplementary Fig. S4. **D**) Observed rate constants for degradation (k_{obs}) for cp8sGFP and rate constant for unfolding (k_u) for eGFP and sGFP substrates, as normalized to WT proteasome. * or ** indicates significant differences from WT ($p < 0.05$ and $p < 0.01$, respectively).

contribute to more efficient engagement of the substrate by the proteasomal motor proteins. Single molecule experiments had shown that a wild-type titin substrate was unfolded at a rate of 1.8 min^{-1} [22], and dihydrofolate reducatase was unfolded at a rate of ~14 min^{-1} unless stabilized by NADPH [23]. The much slower unfolding rates for eGFP and sGFP indicate that the proteasome unfolds substrates at rates that vary over multiple orders of magnitude depending on substrate structure and stability.

We next examined how individual or combinations of YA mutations affected the rate constants for unfolding and degradation. All of the mutants we tested were able to degrade the cp8sGFP substrate, with no evidence of partial degradation or GFP-containing fragment release (Fig. 3A, Supplementary Fig. S2, Supplementary Table S3). Degradation was essentially unaffected for Rpt2 and Rpt6, and moderately slower (3-5-fold) for the remaining single mutants (Fig. 3D), but the modest effects of these mutations were not additive, as Rpt1/3/4 YA (2/1) decreased k_{obs} by only ~2-fold, compared to a predicted ~40-fold additive effect, and the other triple mutants also had small or negligible effects on the observed rate constant. Thus, either mutating individual or multiple aromatic paddles does not affect unfolding of cp8sGFP or degradation of cp8sGFP is so fast that even with multiple mutations unfolding does not become fully rate limiting.

The eGFP substrate was also able to be degraded by all of the mutants we tested (Fig. 3B, Supplementary Fig. S3, Supplementary Table S3). Individual YA mutants had relatively small effects (Fig. 3D) on k_{FL} (all within 2-fold of WT) or on k_u (at most 3-fold). While the Rpt1/3/4 YA (2/1) and the Rpt1/2/6 YA (sequential) reduced the rate of GFP unfolding by only ~3-fold, little different from individual mutations, the alternating Rpt1/4/6 YA mutant reduced k_u by ~7-fold, causing clipping to become more competitive with unfolding and degradation. Although rate constants for tail disengagement and engagement had large errors associated with them, mutants with defects in GFP unfolding also tended to have a lower rate constant for substrate engagement and an equilibrium constant that favored disengagement, suggesting that once fragments are released re-engagement by the proteasome is less likely.

The sGFP substrate was degraded by individual Rpt YA mutants with small effects on k_{FL} (at most up to 2-fold; Supplementary Table S3) but slightly larger effects than seen with eGFP on k_u (2- to 6-fold, other than for Rpt5; Fig. 3D). For Rpt5 YA, there was a clear reduction in the overall rate of degradation of sGFP and the model fit the data well, but there was substantial uncertainty in k_u (0.02 ± 0.1 min^{-1}), which was therefore not statistically significantly different from that observed with WT. In contrast, all three triple-mutants were essentially unable to unfold and degrade GFP (Fig. 3C, Supplementary Fig. S4, Supplementary Table S3). Fits to the model of Fig. 2A gave reductions in k_u of 10-20-fold, but modeling was qualitatively poorer and overestimated the extent of GFP degradation (little to no change in total fluorescence in Fig. 3C and Supplentary Figs. S4G–I). Once unfolding is slowed enough that clipping is the predominant outcome of degradation, it becomes difficult to accurately determine unfolding rates (i.e. there are very large error bars for k_u for all three triple mutants; Fig. 3D).

Defects in unfolding seen with YA mutations could come from the inability to adequately grip the substrate or from effects on the ATPase activity of the proteasome. Previous reports on the effects of individual YA mutations showed that YA mutations could affect the proteasome's ATPase activity, with effects ranging from 0.7 to 2.4-fold, although there was only modest agreement between studies [13,14]. We therefore measured ATPase rates for WT and mutant proteasomes in the absence or presence of substrates (Fig. 4). In the absence of substrate, there was an ~1.5-fold increase in the ATPase rate for the alternating or sequential mutant. However, upon addition of substrates, there were no significant differences between the observed ATPase rates. Thus, although YA mutations can affect ATPase rates, the lack of a substantial change in ATPase rate indicates that the defects in unfolding caused by YA mutations are attributable to defects in the efficiency of pulling by the aromatic paddles rather than the rate of pulling.

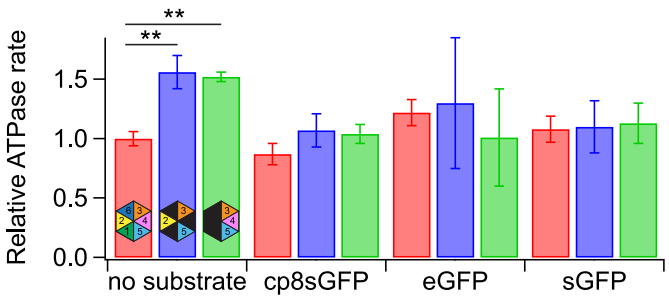

Fig. 4. Relative ATPase rates of WT and mutant proteasome. 20 nM proteasome was assayed ±1 μM substrate. Error bars represent the SEM of 3–5 experiments. ** indicates $p < 0.01$, no other differences were significant ($p > 0.05$).

4. Discussion

Our results indicate that individual Rpt aromatic paddle tyrosines have context-dependent roles in protein unfolding and degradation by the 26S proteasome. Most individual mutations had relatively small effects on either the overall rate of degradation or the rate of GFP unfolding, although these effects generally became larger as the substrate became more difficult to unfold, with some exceptions. For example, in at least partial agreement with previous studies [13,14], mutation of Rpt2 and Rpt6's aromatic paddles have almost no effect on degradation of either the cp8sGFP or eGFP substrate, but the 3-4-fold decrease in unfolding observed with the more stable sGFP substrate reveal that both can play significant roles in degradation when needed. Some mutations had idiosyncratic effects: e.g. Rpt1 affected degradation of cp8sGFP and sGFP, but not eGFP substrates, and appeared to have no effect on cp8sGFP in the context of a triple mutant.

The combination of multiple aromatic paddle mutations further shows the importance of the substrate context. Triple mutants, regardless of arrangement, have little effect on the degradation of cp8sGFP, suggesting that with an impaired proteasome, unfolding, even if reduced, does not become rate-limiting with this substrate. However, there are substantial reductions in the unfolding rate when three alternating subunits have mutant paddles (with smaller reductions with other arrangements). In the hand-over-hand model for aromatic paddle-driven translocation, there are typically four paddles exerting force on the substrate at any point, with one disengaging at the bottom of the staircase and re-engaging at the top of the staircase (Fig. 1B). Alternating WT and mutant paddles would result in good contact with two force-transducing subunits and poor contact with the other two, while three sequential WT paddles followed by three mutant paddles would lead to a continuum from one to three pore loops with good contact. If the force applied per ATP-driven pull is directly proportional to the number of pore loops gripping the substrate, the alternating triple-mutant would have a steady pull at about half the strength of WT, while the sequential triple-mutant or the 2/1 mutant would cycle between pulls from one to three quarters of WT strength. We therefore suggest that stronger pulls are required to unfold eGFP than cp8sGFP, such that the alternating mutant is less likely to unfold eGFP in any given pull than the other triple mutants. The sGFP substrate, which is unable to be unfolded by any of the triple mutants, then either requires four functional paddles pulling at once or a higher proportion of strong pulls for unfolding to occur.

Our results highlight the similarities and differences between unfolding by the proteasome and bacterial ATP-dependent proteases like ClpXP. As with ClpXP [12], the proteasome can better tolerate sequential mutations than alternating mutations. However, our results are consistent with previous work showing the proteasome is a much stronger unfoldase than ClpXP [24]. ClpXP triple YA mutants of any

arrangement were unable to degrade an eGFP substrate, while only the alternating proteasome YA mutant was substantially compromised in eGFP unfolding and degradation. Thus, the proteasome appears to be over-engineered such that it is capable of degrading even very stable proteins. These differences could come from either the motors themselves (which are conserved) or from the structural element domains are pulled against (ie the OB ring in the proteasome).

Finally, kinetic modeling and the inability of proteasome triple YA mutants to degrade sGFP suggests that as a substrate becomes more stable and harder to unfold, a slow tail-clipping reaction (Fig. 2B) in which potential unstructured initiation sites are non-specifically removed will eventually outcompete unfolding. This competition suggests that kinetic proofreading is being used to ensure that substrates that are too stable for the proteasome to unfold (i.e. those that persist too long at the proteasome without being fully degraded) do not tie up the proteasome and prevent it from degrading other waiting client proteins. Kinetic proofreading may be particularly important when the proteasome encounters aggregated proteins, which might otherwise be engaged in many futile rounds of attempted unfolding.

Funding

This work was supported by the National Science Foundation (Grant No. 1935596) and the Research Corporation for Scientific Advancement (Grant No. 23334).

Declaration of competing interest

The authors declare the following financial interests/personal relationships which may be considered as potential competing interests: Daniel A. Kraut reports financial support was provided by National Science Foundation. Daniel A. Kraut reports financial support was provided by Research Corporation for Scientific Advancement.

Acknowledgements

The authors would like to thank Dr. Aimee Eggler and members of the Kraut lab for helpful discussions and feedback.

Appendix A. Supplementary data

Supplementary data to this article can be found online at https://doi.org/10.1016/j.bbrc.2023.08.025.

References

[1] S. Zhang, Y. Mao, AAA+ ATPases in protein degradation: structures, functions and mechanisms, Biomolecules 10 (2020) 629.
[2] Y. Mao, Structure, dynamics and function of the 26S proteasome, Subcell. Biochem. 96 (2021) 1–151.
[3] J.A.M. Bard, E.A. Goodall, E.R. Greene, E. Jonsson, K.C. Dong, A. Martin, Structure and function of the 26S proteasome, Annu. Rev. Biochem. 87 (2018) 697–724.
[4] S.N. Gates, A. Martin, Stairway to translocation: AAA+ motor structures reveal the mechanisms of ATP-dependent substrate translocation, Protein Sci. 29 (2019) 407–419.
[5] A.H. de la Peña, E.A. Goodall, S.N. Gates, G.C. Lander, A. Martin, Substrate-engaged 26S proteasome structures reveal mechanisms for ATP-hydrolysis-driven translocation, Science 362 (2018), eaav0725.
[6] Y. Dong, S. Zhang, Z. Wu, X. Li, W.L. Wang, Y. Zhu, S. Stoilova-McPhie, Y. Lu, D. Finley, Y. Mao, Cryo-EM structures and dynamics of substrate-engaged human 26S proteasome, Nature 565 (2019) 49–55.
[7] R.T. Sauer, T.A. Baker, AAA+ proteases: ATP-fueled machines of protein destruction, Annu. Rev. Biochem. 80 (2011) 587–612.
[8] E. Park, Y.M. Rho, O.-J. Koh, S.W. Ahn, I.S. Seong, J.-J. Song, O. Bang, J.H. Seol, J. Wang, S.H. Eom, C.H. Chung, Role of the GYVG pore motif of HslU ATPase in protein unfolding and translocation for degradation by HslV peptidase, J. Biol. Chem. 280 (2005) 22892–22898.
[9] T. Yamada-Inagawa, T. Okuno, K. Karata, K. Yamanaka, T. Ogura, Conserved pore residues in the AAA protease FtsH are important for proteolysis and its coupling to ATP hydrolysis, J. Biol. Chem. 278 (2003) 50182–50187.
[10] J. Hinnerwisch, W.A. Fenton, K.J. Furtak, G.W. Farr, A.L. Horwich, Loops in the central channel of ClpA chaperone mediate protein binding, unfolding, and translocation, Cell 121 (2005) 1029–1041.
[11] A. Martin, T.A. Baker, R.T. Sauer, Pore loops of the AAA+ ClpX machine grip substrates to drive translocation and unfolding, Nat. Struct. Mol. Biol. 15 (2008) 1147–1151.
[12] O. Iosefson, A.R. Nager, T.A. Baker, R.T. Sauer, Coordinated gripping of substrate by subunits of a AAA+ proteolytic machine, Nat. Chem. Biol. 11 (2015) 201–206.
[13] J. Erales, M.A. Hoyt, F. Troll, P. Coffino, Functional asymmetries of proteasome translocase pore, J. Biol. Chem. 287 (2012) 18535–18543.
[14] R. Beckwith, E. Estrin, E.J. Worden, A. Martin, Reconstitution of the 26S proteasome reveals functional asymmetries in its AAA+ unfoldase, Nat. Struct. Mol. Biol. 20 (2013) 1164–1172.
[15] D.M. Rubin, M.H. Glickman, C.N. Larsen, S. Dhruvakumar, D. Finley, Active site mutants in the six regulatory particle ATPases reveal multiple roles for ATP in the proteasome, EMBO J. 17 (1998) 4909–4919.
[16] M.F. Laughery, T. Hunter, A. Brown, J. Hoopes, T. Ostbye, T. Shumaker, J. J. Wyrick, New vectors for simple and streamlined CRISPR–Cas9 genome editing in Saccharomyces cerevisiae, Yeast 32 (2015) 711–720.
[17] B.L. Schneider, W. Seufert, B. Steiner, Q.H. Yang, A.B. Futcher, Use of polymerase chain reaction epitope tagging for protein tagging in Saccharomyces cerevisiae, Yeast 11 (1995) 1265–1274.
[18] C.E. Bragança, D.A. Kraut, Mode of targeting to the proteasome determines GFP fate, J. Biol. Chem. 295 (2020) 15892–15901.
[19] C.M. Hurley, D.A. Kraut, Determination of proteasomal unfolding ability, Methods Mol. Biol. 2365 (2021) 217–244.
[20] S. Hoops, S. Sahle, R. Gauges, C. Lee, J. Pahle, N. Simus, M. Singhal, L. Xu, P. Mendes, U. Kummer, COPASI–a COmplex PAthway SImulator, Bioinformatics 22 (2006) 3067–3074.
[21] Y. Saeki, E. Isono, A. Toh-E, Preparation of ubiquitinated substrates by the PY motif-insertion method for monitoring 26S proteasome activity, Methods Enzymol. 399 (2005) 215–227.
[22] J.A.M. Bard, C. Bashore, K.C. Dong, A. Martin, The 26S proteasome utilizes a kinetic gateway to prioritize substrate degradation, Cell 177 (2019) 286–298.
[23] D.A. Kraut, E. Israeli, E.K. Schrader, A. Patil, K. Nakai, D. Nanavati, T. Inobe, A. Matouschek, Sequence- and species-dependence of proteasomal processivity, ACS Chem. Biol. 7 (2012) 1444–1453.
[24] P. Koodathingal, N.E. Jaffe, D.A. Kraut, S. Prakash, S. Fishbain, C. Herman, A. Matouschek, ATP-Dependent Proteases Differ Substantially in Their Ability to Unfold Globular Proteins, vol. 284, 2009, pp. 18674–18684.